A comprehensive study of texture analysis based on local binary patterns

Rodrigo Nava[a], Gabriel Cristóbal[b] and Boris Escalante-Ramírez[c]

[a]Posgrado en Ciencia e Ingeniería de la Computación, Universidad Nacional Autónoma de México, Mexico City, Mexico.
[b]Instituto de Óptica, Spanish National Research Council (CSIC), Serrano 121, Madrid 28006, Spain.
[c]Departamento de Procesamiento de Señales, Facultad de Ingeniería, Universidad Nacional Autónoma de México, Mexico City, Mexico.

ABSTRACT

One of the main goals of texture analysis is to provide a robust mathematical description of the spatial behavior of intensity values in any given neighborhood. These local distributions –called textures– characterize object surfaces and are used for pattern identification and recognition of images. However, some spatial patterns may vary from quite simple stripes to randomness, where textures look like unstructured noise. Since textures can exhibit a large number of properties such as surface materials and geometry of the lighting sources, many different approaches have been proposed. A featured method is the modification of Wang's algorithm made by Ojala et al, the so-called local binary patterns (LBP). The LBP algorithm uses a 3×3 square mask named "texture spectrum" which represents a neighborhood around a central pixel. The values in the square mask are compared with the central pixel and then multiplied by a weighting function according with their positions. This technique has become popular due to its computational simplicity and more importantly for encoding a powerful signature for describing textures. Specially, it has gained increased importance in image classification, where the success not only depends on a robust classifier but also relies in a good selection of the feature descriptors. However, Ojala's algorithm presents some limitations such as noise sensitivity and lack of invariance to rotational changes. This fact has fostered many extensions of the original LBP approach that in many cases are based on minor changes in order to attain e.g. illumination and rotational invariance or improving the robustness to noise. In this paper we present a detailed overview of the LBP algorithm and other recently modifications. In addition, we perform a texture classification study with seven algorithms in presence of rotational changes, noise degradation, contrast information, and different sizes of LBP masks using the USC-SIPI database. The LBP histograms have been evaluated using the Kullback-Leibler distance. This study will be a valuable insight for establishing a robust and efficient texture descriptor to solve real world problems.

Keywords: Local binary patterns, texture analysis, texture classification, distance measure, USI-SIPI, Brodatz

1. INTRODUCTION

Many methods of analysis characterize textures in terms of their intrinsic features but given the fact that textures are quite varied, the algorithms not only depend on studying the images but also on the goal for which the image texture is used. Since texture is a fundamental image property composed of repetitive patterns that describes a perceptually homogeneous region, it has been studied in the fields of visual perception and computer vision. Commonly, it is used in early stages of the visual information processing, especially for classification and segmentation purposes.[1]

Further author information: (Send correspondence to R.N.)
R.N.: E-mail: urielrnv@uxmcc2.iimas.unam.mx
B.E.: E-mail: boris@servidor.unam.mx, Telephone: (52) 55-56161719
G.C.: E-mail: gabriel@optica.csic.es, Telephone: (34) 91-5616800 (x942319), Fax: (34) 91-5645557

Optics, Photonics, and Digital Technologies for Multimedia Applications II, edited by
Peter Schelkens, Touradj Ebrahimi, Gabriel Cristóbal, Frédéric Truchetet, Pasi Saarikko,
Proc. of SPIE Vol. 8436, 84360E · © 2012 SPIE · CCC code: 0277-786X/12/$18 · doi: 10.1117/12.923558

Downloaded from SPIE Digital Library on 03 May 2012 to 161.111.24.211. Terms of Use: http://spiedl.org/terms

Although textures are widely used as descriptors, it has been difficult to establish an appropriate definition. Many vision researchers have given definitions frequently in the context of different applications areas. Approaches to texture analysis are usually categorized into: *i*) **statistical methods:** these methods analyze spatial distribution of pixels using features taken from the first and second-order histograms based on the assumption that the intensity variations are more or less constants within a region and take greater values outside their boundary.[2] Inside of this group one can highlight the features extracted from the co-occurrence matrix.[3] *ii*) **spectral methods:** these methods collect a distribution of filter responses for a further classification. A comparative study can be found in Randen et al.[4] Many algorithms in this category are focused on face recognition classification.[5] In particular, Gabor filters have proven to be powerful and precise for describing texture patterns.[6] *iii*) **structural methods:** textures are characterized by a set of primitives which are organized according to a certain placement rule. The placement rule defines the spatial relationship among primitives and may be expressed in terms of adjacencies. *iv*) **stochastic methods:** these methods assume that textures are the realization of stochastic processes and estimate the associated parameters, e.g., Seetharaman uses a Bayesian approach as a texture descriptor.[7]

Recent trends in texture classification attempt to unify the concepts of statistical and structural approaches. Ojala[8] observed that these two concepts have complementary characteristics that allow modeling textures as distributions of *texture units*. The LBP operator proposed by Ojala[8] is a two-level version from the Wang's work[9] which compare the values in a square mask against a the central pixel. This operator belongs to a group of non-parametric local transformations that are distinguished by the use of ordered information among data. Non-parametric local transformations are local transformations that rely on the relative order of pixel values. They transform an image into an array of integer labels, (see Fig. 2) and encode the pixel-wise information of the textures as a histogram. This histogram can be interpreted as the fingerprint of the analyzed object.

Similarly to the Ojala's work, Zabih[10] proposed two alternative non-parametric local transforms. The first transform called rank transform (RT) is defined as the number of pixels in a local square region that are lesser that the value of a central pixel. The second non-parametric local transform named census transform (CT) maps the local square neighborhood into a bit string representing the set of neighbor pixels that are lesser than a central pixel value. Both RT and CT depend solely on a set of pixel comparisons. Nevertheless, the first limitation of these kind of methods is that the amount of information associated to a pixel is not very large which induces noise sensitivity. Another limitation is that the local measures rely heavily upon the intensity of a central pixel. However, the last drawback can avoid by doing comparisons using local means or median values instead of central pixel intensities.

After the initial LBP proposal, many modifications and improvements have emerged in the literature, most of them are related to face analysis where it is assumed that input faces are registered. For a thorough description of LBP operators see two recent surveys and a book monograph.[5,11,12]

In this paper we present a detailed overview of the original LBP algorithm as well as the most significant extensions that have been proposed in the literature from theoretical to practical perspective. In Section 3 we perform an assessment of seven algorithms in presence of rotational changes, noise degradations, contrast information, and different sizes of LBP masks using the USC-SIPI database. This study includes classification tests using KL distance. Finally, conclusions are drawn in Section 4.

2. LOCAL BINARY PATTERN METHODS

The very first approach to LBP was given by Ojala[8] and is based on the idea that textural properties within homogeneous regions can be mapped into patterns which represent micro-features. The LBP proposal uses a 3×3 square mask called "texture spectrum" which represents a neighborhood around a central pixel, Fig. 1(a). The values in the square mask are compared with the central pixel, those ones lesser than the central value are labeled with "0" otherwise they are labeled with "1", Fig.1(b). The labeled pixels are multiplied by a weighting function according with their positions to form a pattern chain, Fig. 1(c). Afterward, the values of the eight pixels are summed to obtain a label for this neighborhood, Fig. 1(d), this method produced 2^8 possible labels.

Ojala claimed that this type of threshold provides a robust way for describing local texture patterns. However, Tan[13] have revisited the original approach and demonstrated that a generalization of LBP called local ternary patterns (LTP) is more discriminant and less sensitive to noise for texture analysis.

Downloaded from SPIE Digital Library on 03 May 2012 to 161.111.24.211. Terms of Use: http://spiedl.org/terms

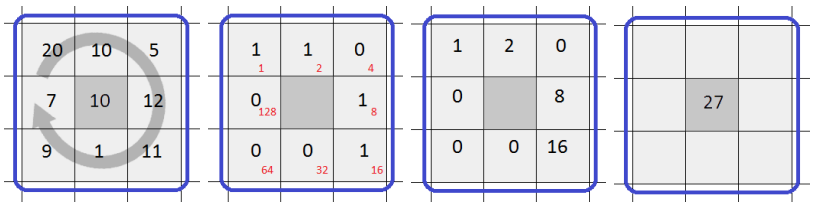

Figure 1. Based on a square mask of 3×3 the LBP algorithm computes a label by comparisons between a central pixel and its surrounding neighbors. This method produces 2^8 possible labels. In this example, we chose a circular path to visit all the pixels but in the original proposal the order to visit all the pixels is per row. Hence the central value is $p_c = 10$ and the final label will be 27.

Finally, after this process is completed for the whole image, a histogram is computed so that can be interpreted as a fingerprint of the analyzed object. Although this method provides information about local spatial structures, it is not invariant to rotational changes and does not include contrast information which has been demonstrated to be crucial to improve the discrimination of some textures.

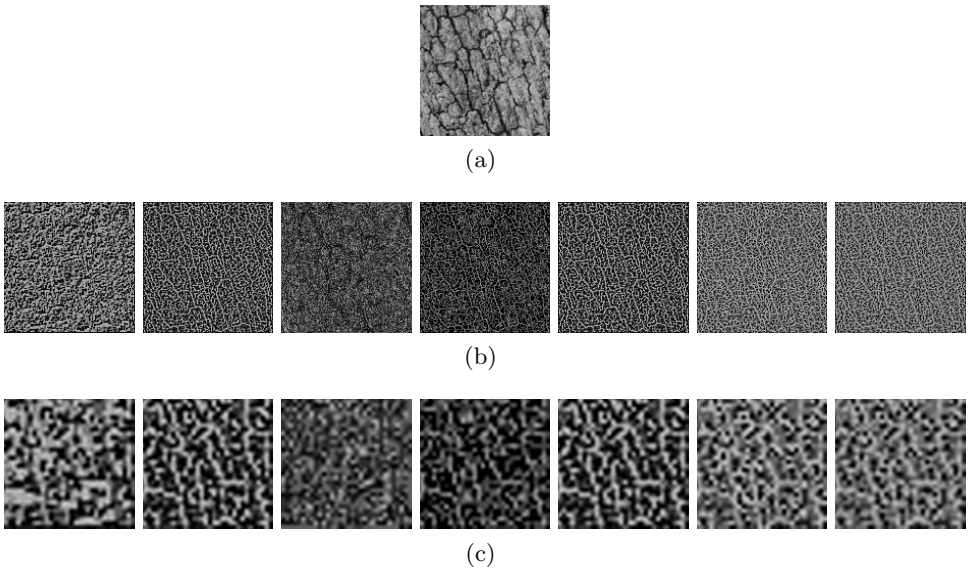

Figure 2. Many methods based on the original LBP algorithm have emerged in the literature. Using Bark texture (D12) in Fig. 2(a), we show in Fig. 2(b) seven LBP-images. From left to right: LBP, $LBP^{min}_{P,R}$, $LBP^{ni}_{P,R}$, $LBP^{med}_{P,R}$, $LBP^{dom}_{P,R}$, $LBP^{uni}_{P,R}$, and $LBP^{num}_{P,R}$ respectively. Fig. 2(c) results are magnified by a factor of 4 for a better visualization.

2.1 Modifications of the local binary pattern method

In this work, a wide set of LBP methods are analyzed. Here, we summarize the main characteristics of the algorithms selected in the current study. In particular, this study is focused in analyzing LBP algorithms that provide rotational invariance for their direct implication in practical applications.

- ◇ Ojala proposed a generalization of his own operator.[14] Such generalization can be obtained using a circular neighborhood denoted by (P, R) where P represents the number of sampling points and R represents the radius of the neighborhood. The sampling point coordinates (x_p, y_p) are calculated using the expression $\left(x_c + R\cos\left(\frac{2\pi p}{P}\right), y_c - R\sin\left(\frac{2\pi p}{P}\right)\right)$. When the sampling coordinates do not fall at integer positions, the intensity values are bilinearly interpolated. This implementation is called circular LBP ($LBP_{P,R}$).

$$LBP_{P,R}(g_c) = \sum_{p=0}^{P-1} s(g_p - g_c)\, 2^p \tag{1}$$

Downloaded from SPIE Digital Library on 03 May 2012 to 161.111.24.211. Terms of Use: http://spiedl.org/terms

where g_c is the central pixel at (x_c, y_c) coordinates and $\{g_p | p = 0, \ldots, P-1\}$ are the values of the neighbors. The comparison function $s(x)$ is defined as:

$$s(x) = \begin{cases} 1 & \text{if } x \geq 0 \\ 0 & \text{if } x < 0 \end{cases} \tag{2}$$

Eq. (1) represents a "texture unit" composed of $P+1$ elements (central pixel included). There are 2^P possible texture units describing spatial patterns in a neighborhood of P points. In addition, $LBP_{P,R}$ achieves invariance against any monotonic transformation by considering the sign of the differences in $s(g_p - g_c)$.

◇ Pietikäinen proposed a modification called rotation invariant LBP ($LBP^{min}_{P,R}$) in order to minimize the effects of rotation.[15] The main idea is to apply a circular shift to find the minimum value that the pattern chain may represents, see Eq. (3). This approach identifies 36 different values when using $P = 8$. However, the Eq. (3) only achieves invariance in a discrete digital domain because only for 90° perfect rotation invariance can be achieved.

$$LBP^{min}_{P,R}(g_c) = min\{ROR(LBP_{P,R}(g_c), i) | i = 0, \ldots, P-1\} \tag{3}$$

where $ROR(x, i)$ performs a circular bit-wise right shift operation i times.

◇ Ojala observed that over 90% of texture patterns can be described with few spatial transitions, which are the changes (0/1) in the pattern chain.[14] He introduced a uniformity measure $U(LBP_{P,R}(g_c))$ which corresponds to the number of spatial transitions as follows:

$$U(LBP_{P,R}(g_c)) = |s(g_{p-1} - g_c) - s(g_0 - g_c)| + \sum_{p=1}^{P-1} |s(g_p - g_c) - s(g_p - g_c)| \tag{4}$$

In this way, the uniform LBP ($LBP^{uni}_{P,R}$) can be obtained as:

$$LBP^{uni}_{P,R}(g_c) = \begin{cases} \sum_{p=0}^{P-1} s(g_p - g_c) & \text{if } U(LBP_{P,R}(g_c)) \leq 2 \\ P+1 & \text{otherwise} \end{cases} \tag{5}$$

◇ Yan Ma[16] proposed the number LBP ($LBP^{num}_{P,R}$) as an extension of the Eq. (5) by dividing the non-uniform patterns into groups based on the number of "1" or "0" bits as follows:

$$LBP^{num}_{P,R}(g_c) = \begin{cases} \sum_{p=0}^{P-1} s(g_p - g_c) & \text{if } U(LBP_{P,R}(g_c)) \leq 2 \\ Num_1\{LBP_{P,R}(g_c)\} & \text{if } \begin{array}{l} U(LBP_{P,R}) > 2 \quad \text{and} \\ Num_1\{LBP_{P,R}(g_c)\} \geq Num_0\{LBP_{P,R}(g_c)\} \end{array} \\ Num_0\{LBP_{P,R}(g_c)\} & \text{if } \begin{array}{l} U(LBP_{P,R}) > 2 \quad \text{and} \\ Num_1\{LBP_{P,R}(g_c)\} < Num_0\{LBP_{P,R}(g_c)\} \end{array} \end{cases} \tag{6}$$

where $Num_1\{\bullet\}$ is the number of "1" and $Num_0\{\bullet\}$ is the number of "0" in the non-uniform pattern.

◇ Liu stated that the likelihood of a central pixel only depends on its neighbors.[17]Hence, the neighbor-intensity LBP ($LBP^{ni}_{P,R}$) can be obtained by replacing the central pixel with the average of its neighbors as follows:

$$LBP^{ni}_{P,R}(g_c) = \sum_{p=0}^{P-1} s(g_p - \mu) 2^p \tag{7}$$

Downloaded from SPIE Digital Library on 03 May 2012 to 161.111.24.211. Terms of Use: http://spiedl.org/terms

where

$$\mu = \frac{1}{P}\sum_{p=0}^{P-1} g_p \tag{8}$$

◇ The presence of noise can seriously impair the performance of the LBP operator. Zabih's proposal[10] replaces the central pixel with the median of itself and the P neighbors.

$$LBP_{P,R}^{med}(g_c) = \sum_{p=0}^{P-1} s(g_p - \widetilde{g}) \tag{9}$$

where $\widetilde{g}$ represents the median of the P neighbors and the central pixel. This modification is still invariant to rotation but less sensitive to noise. It is also invariant to monotonic illumination changes.

◇ Fu and Wei[18] addressed the problem of noise by considering that in most cases the central pixels provide more information than their neighbor counterparts. They redefined Eq. (2) as:

$$s(x) = \begin{cases} 1 & |x| \geq c \\ 0 & |x| < c \end{cases} \tag{10}$$

where c is a fixed threshold.

Fu and Wei proposed the centralized LBP ($LBP_{P,R}^{cen}$) as follows:

$$LBP_{P,R}^{cen}(g_c) = \sum_{p=0}^{\frac{P}{2}-1} s\left(g_p - g_{p+\frac{P}{2}}\right) 2^p + s(g_c - g_{tot})\, 2^{\frac{p}{2}} \tag{11}$$

and g_{tot} is defined as:

$$g_{tot} = \frac{1}{P+1}\left(g_c + \sum_{p=0}^{P-1} g_p\right) \tag{12}$$

Due to the fact that the algorithm considers correlation between opposite pixel points, this algorithm is not invariant to rotation.

◇ Tan proposed an extension called extended LBP ($LBP_{P,R}^{ext}$) by using the value of central pixels plus a tolerance interval t as local threshold.[19] t is a user-specific value, usually set at "1". Each pixel in the interval $g_c \pm t$ is quantized as zero. Pixels above the tolerance interval are labeled with "1" and those below the interval are labeled with "−1" as follows:

$$s(x) = \begin{cases} 1 & \text{if } x > t \\ 0 & \text{if } |x| \leq t \\ -1 & \text{if } x < -t \end{cases} \tag{13}$$

here x is the difference between the P neighbors and their central pixel. Each ternary pattern is split into upper and lower patterns and each part is encoded as a separate LBP pattern. Finally, their histograms are concatenated.

◇ Guo[20] suggested to consider both the sign and magnitude of a d_p vector to form the completed LBP ($LBP_{P,R}^{com}$). In Eq. (1), only the sign component is considered. Here, $d_p = \{g_p - g_c | p = 0, 1, \ldots, P-1\}$ is split into two components as follows:

$$d_p = s_p * m_p = \begin{cases} s_p & = sign(d_p) \\ m_p & = |d_p| \end{cases} \tag{14}$$

where s_p and m_p are the sign and magnitude of d_p respectively.

Downloaded from SPIE Digital Library on 03 May 2012 to 161.111.24.211. Terms of Use: http://spiedl.org/terms

◇ Liao proposed the dominant LBP ($LBP^{dom}_{P,R}$) which is a modification of Eq. (5) based on the fact that $LBP^{uni}_{P,R}$ in practice is not well suited to encode some complicated pattern textures such as curvature edges and crossing boundaries of corners.[21] A possible explanation is due to the fact that the extracted uniform patterns do not have a dominant proportion of them to better represent the object (or image). Liao et al. have shown that given a set of training images, the required number of patterns to better representing textures corresponds to at least 80% of the pattern occurrences. The first step of their procedure is to compute the histogram and sort it in descending order. The second step is to extract a vector to obtain the 80% of pattern occurrences. This procedure guarantees a suitable framework for representing textures.

◇ Previously, Ojala[14] proposed the use of a joint representation $LBP_{P,R}/VAR_{P,R}$, where $VAR_{P,R}$ represents the local variance. However, $VAR_{P,R}$ has continuous values. Therefore, it has to be quantized. Guo[22] included complementary information of the local contrast in a new scheme called local binary pattern variance ($LBPV_{P,R}$).

A rotation invariant measure of the local variance can be defined as:

$$VAR_{P,R}(g_c) = \frac{1}{P}\sum_{p=0}^{P-1}(g_p - u)^2 \tag{15}$$

where $\{g_p|p = 0, \ldots, P-1\}$ are the g_c neighbors and $u = \frac{1}{P}\sum_{p=0}^{P-1} g_p$.

Calculation of the LBP histogram does not include the information of variance $VAR_{P,R}$. The $LBPV_{P,R}$ descriptor offers a solution for that as follows:

$$LBPV_{P,R}(k) = \sum_{i=1}^{N}\sum_{j=1}^{M}\omega\left(LBP_{P,R}(i,j), k\right), k \in [0, K] \tag{16}$$

$$\omega\left(LBP_{P,R}(i,j), k\right) = \begin{cases} VAR_{P,R}(i,j) & LBP_{P,R}(i,j) = k \\ 0 & \text{otherwise} \end{cases} \tag{17}$$

The variance $VAR_{P,R}$ can be used as an adaptive weight to adjust the contribution of the LBP code in the histogram calculation.

The advantage of the $LBP_{P,R}/VAR_{P,R}$ scheme is the use of both local spatial and contrast information and the quantization of the variance can be done by the distribution of values into N bins with an equal number of entries. Another option is to distribute all the quantized variance values into histograms with the same number of bins that the LBP histogram. It is important to consider that too few bins will fail to provide enough discriminative information while too many bins may lead to sparse and unstable histograms.

3. ASSESSMENT RESULTS

The experimental tests were performed using the USC-SIPI image database available at.[23] This database consists of thirteen grayscale textures of 512×512 pixels. The textures bark (D12), brick (D94), bubbles (D112), grass (D9), leather (D24), pigskin (D92), raffia (D84), sand (D29), straw (D15), water(D38), weave (D16), wood (D68), and wool (D19) –the number between parenthesis is the identification number in the Brodatz texture book[24]– were digitized at seven different rotation angles: 0, 30, 60, 90, 120, 150, and 200 degrees. The USC-SIPI image database provide a hardware-rotated subset of textures avoiding in this way the introduction of artifacts if the rotation is performed by software. For purposes of efficiency, all images were rescaled at 64×64 and 128×128 pixels with 8 bits/pixel using bicubic interpolation.

In this evaluation set, we consider seven rotation invariant descriptors: LBP^{min}, $LBP^{min}_{P,R}$, $LBP^{ni}_{P,R}$, $LBP^{med}_{P,R}$, $LBP^{dom}_{P,R}$, $LBP^{uni}_{P,R}$, and $LBP^{num}_{P,R}$ from the list of methods described in Section 2. Furthermore, we distinguish two subsets: *i*) $LBP^{min}_{P,R}$, $LBP^{ni}_{P,R}$, $LBP^{med}_{P,R}$, and $LBP^{dom}_{P,R}$ which are modifications of the LBP^{min} approach. The methods in this subset compute the LBP labels based on the pattern chain values and their final histograms

Downloaded from SPIE Digital Library on 03 May 2012 to 161.111.24.211. Terms of Use: http://spiedl.org/terms

is of 36 bins length. *ii)* $LBP^{num}_{P,R}$ is a refined model of $LBP^{uni}_{P,R}$. These methods compute the LBP labels based on the number of transitions of the pattern chains.

In order to evaluate the robustness of the algorithms against rotational changes, we calculated the mean and variance features of each reference LBP (non-rotated textures) and compare against its rotated versions. We used a normalized measure of dispersion C_v and computed the statistical variations among the orientations as follows:

$$C_v = \frac{\sigma}{\mu} \tag{18}$$

where σ and μ are the standard deviation and mean for each feature respectively. The lower coefficient the higher robustness against rotation changes.

Table 1 shows the coefficients of variation for the two groups of images (64×64 and 128×128 respectively). μ_{64} and σ^2_{64} represents the mean and the variance of test images of 64×64 pixels and μ_{128} and σ^2_{128} represents the mean and the variance of the test images of 128×128 pixels respectively.

Table 1. The slight numerical variations of the C_v indicates the robustness of the the extracted features. The lower the coefficient of variation the higher the robustness to rotation changes.

	LBP^{min}	$LBP^{min}_{P,R}$	$LBP^{ni}_{P,R}$	$LBP^{med}_{P,R}$	$LBP^{dom}_{P,R}$	$LBP^{uni}_{P,R}$	$LBP^{num}_{P,R}$
μ_{64}	0.0104	0.0057	0.0162	0.0100	0.0100	0.0071	**0.0049**
σ^2_{64}	**0.0094**	0.0175	0.0321	0.0350	0.0350	0.0303	0.0329
μ_{128}	0.0089	0.0053	0.0089	0.0050	0.0050	0.0046	**0.0033**
σ^2_{128}	**0.0086**	0.0122	0.0222	0.0299	0.0299	0.0275	0.0241

We should note that LBP^{min} and $LBP^{min}_{P,R}$ differ that the first one does not use interpolated neighbors but the second one does. Interpolated neighbors minimize the feature mean μ but increase the variance σ^2.

3.1 Kullback-Leibler distance

Since LBP histograms act as fingerprints of textures, it is possible to consider them as similarity measures among all different textures. Although the Kullback-Leibler divergence (KL) –a generalization of Shannon's entropy– is not a true metric rather it is a relative entropy measure, it can be used as a suitable metric for measuring distances between histograms as follows:

$$D_{KL}(A, B) = \sum_{i=0}^{b-1} P_i(B) \log \frac{P_i(B)}{P_i(A)} \tag{19}$$

where A and B are two histograms with b bins length each, and P_i denotes the probability of the i bin.

The classification procedure setup consisted of comparing histogram distance of each reference image against all rotated images, (see Table 2). This experiment was performed both for testing images of 64×64 and 128×128 pixels.

The classification rates are consistent with those reported in the literature. Pietikäinen[15] reported an error rate of 38.5% for the LBP^{min} algorithm. Here, we got 38.46%. The best classification rate is achieved with the $LBP^{dom}_{P,R}$, one possible reason is that this approach rules out 20% of patterns that in many cases can be interpreted as noise.

3.2 Noise sensitivity

LBP algorithms are very sensitive to noise, specially when a small neighborhood is used. Since the amount of information associated to a pixel is not very large, even a small change in any pixel value could lead to a different label. Table 3 shows the classification performance of the noisy images of 128×128 pixels. The seven algorithms have been evaluated with the addition of Gaussian noise with mean $\mu = 0$ and standard deviation $\sigma = 0.1$ and under the effects of Poisson noise. These noise algorithms were implemented with the Matlab *imnoise* function. According with Table 3 and for the images analyzed, $LBP^{dom}_{P,R}$ performed best for Gaussian noise and $LBP^{ni}_{P,R}$ for Poisson noise.

Downloaded from SPIE Digital Library on 03 May 2012 to 161.111.24.211. Terms of Use: http://spiedl.org/terms

Table 2. Comparison of texture classification using the KL distance.

Scheme	64×64		128×128		References
	# textures	Accuracy rate (%)	# textures	Accuracy rate (%)	
LBP^{min}	56	61.54	66	72.53	[15]
$LBP^{min}_{P,R}$	53	58.24	63	69.23	[15]
$LBP^{ni}_{P,R}$	57	62.64	65	71.43	[17]
$LBP^{med}_{P,R}$	54	59.34	71	78.02	[10]
$LBP^{dom}_{P,R}$	**68**	**74.73**	**73**	**80.22**	[21]
$LBP^{uni}_{P,R}$	67	73.63	**73**	**80.22**	[14]
$LBP^{num}_{P,R}$	63	69.23	**73**	**80.22**	[16]

3.3 Adding variance information

Illumination variations are one of the most important challenges for the current feature descriptors. Tan[13] claims that LBP performance decreases almost exponentially under extreme conditions. The LBP by itself is only invariant to monotonic illumination changes and does not entail the contrast information of textures which is important in the discrimination.

In the next experiment we used the Eq. 15 for computing the local variance information of the test images. Here we are interested in combined information of both LBP and local variance $VAR_{P,R}$ features. However, $VAR_{P,R}$ produces continuous values which need to be quantized. Ojala proposed to quantize variance values so that all bins have an equal number of elements.[8] So far, establishing the number of bins is still an open issue.

LBP and $VAR_{P,R}$ histograms could be combined in two ways: jointly or mixed,.[20] In the first one, similar to 2D joint histograms, we can build a 3D joint histogram of them. In the second way, a large histogram is built by concatenating both LBP and $VAR_{P,R}$ histograms to form the so-called "pseudo joint histogram".

Table 4 shows classification rates of LBP algorithms with and without $VAR_{P,R}$ information on images of size 128×128. Here we used pseudo joint histogram.

As we expected, the results obtained with joint pairs of features provide the best performances with error rates around 7.70%. This emphasizes the importance of using other features besides the LBP operator. In fact, if we consider only the local variance $VAR_{P,R}$ as a feature descriptor, the classification rate reaches 86.81%.

In the next Fig. 3 we present a performance comparison between $LBP^{uni}_{P,R}$ and $LBP^{uni}_{P,R} \backslash VAR_{P,R}$ approaches. There is a strong indication that the local variance is more discriminant than LBP features themselves in the

Table 3. Performance of LBP approaches under additive Gaussian noise with media $\mu = 0$ and $\sigma^2 = 0.1$ and under Poisson noise.

Scheme	Gaussian noise		Poisson noise	
	# textures	Accuracy rate (%)	# textures	Accuracy rate (%)
LBP^{min}	55	60.44	71	78.02
$LBP^{min}_{P,R}$	52	57.14	66	72.53
$LBP^{ni}_{P,R}$	51	56.04	**73**	**80.22**
$LBP^{med}_{P,R}$	53	58.24	74	81.32
$LBP^{dom}_{P,R}$	**61**	**67.03**	69	75.82
$LBP^{uni}_{P,R}$	60	65.93	69	75.82
$LBP^{num}_{P,R}$	51	56.04	51	56.04

Downloaded from SPIE Digital Library on 03 May 2012 to 161.111.24.211. Terms of Use: http://spiedl.org/terms

Table 4. Comparison of texture classification including local variance information.

Scheme	LBP only		$VAR_{P,R}$	
	# textures	Accuracy rate (%)	# textures	Accuracy rate (%)
LBP^{min}	66	72.53	76	83.51
$LBP^{min}_{P,R}$	63	69.23	81	89.01
$LBP^{ni}_{P,R}$	65	71.43	81	89.01
$LBP^{med}_{P,R}$	71	78.02	80	87.91
$LBP^{dom}_{P,R}$	**73**	**80.22**	81	89.01
$LBP^{uni}_{P,R}$	**73**	**80.22**	**84**	**92.30**
$LBP^{num}_{P,R}$	**73**	**80.22**	82	90.10

classification process. A Fischer discriminant score[25] will allow to select the most informative features by rejecting those noisy features.

3.4 Neighborhood size

Another important issue of the original LBP is the neighborhood size. The next experiment was aimed to assess the radius size influence in texture classification. Table 5 presents the classification performance of the seven LBP approaches with radius $R = \{1, 2, 3\}$ on images of size 128×128.

Table 5. Comparison of texture classification using different neighborhood size.

Scheme	$R = 1$	$R = 2$	$R = 3$
$LBP^{min}_{P,R}$	63	71	56
$LBP^{ni}_{P,R}$	65	71	**70**
$LBP^{med}_{P,R}$	71	64	57
$LBP^{dom}_{P,R}$	**73**	**74**	67
$LBP^{uni}_{P,R}$	**73**	72	**70**
$LBP^{num}_{P,R}$	**73**	68	63

For the subset one, the highest classification rate was achieved with $R = 2$ while higher radius size caused poor classification rates. On the contrary, for the subset two, (the last two methods of Table 5), the best rates was achieved with $R = 1$.

4. CONCLUSIONS

The main goal of this study was to perform a comparative study of several LBP approaches because this concept has represented a milestone in texture analysis. The LBP descriptors have been powerful tools for feature encoding. They have been successfully used in many different image analysis applications, in particular in the area of face recognition due to their excellent properties and computational simplicity. Since the original LBP proposal has many limitations such as noise sensibility and it is affected by rotational transforms, a large number of extensions have been proposed. Here, we presented a wide overview of the most important LBP approaches proposed in the literature and performed evaluation tests for texture classification of seven algorithms in presence of rotational changes, noise degradation, contrast information, and different sizes of LBP masks using the USC-SIPI database. Although in general, the classification rates of the seven LBP's are poor, starting from 58.24% up to 80.22%, the results obtained with joint pairs of features, both LBP and local variance, provide the best performances with error rates around 7.7%. However, due to their lack of strength against noise and non-uniform illumination changes, it needs a pre-processing step (filtering) as a previous stage to increase their robustness.

Downloaded from SPIE Digital Library on 03 May 2012 to 161.111.24.211. Terms of Use: http://spiedl.org/terms

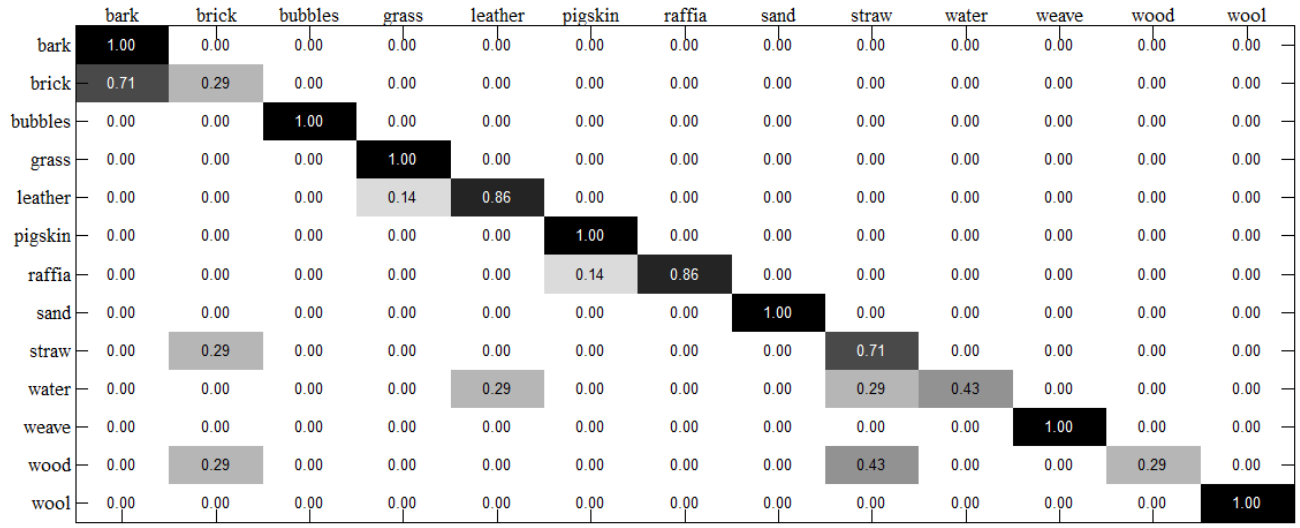

(a)

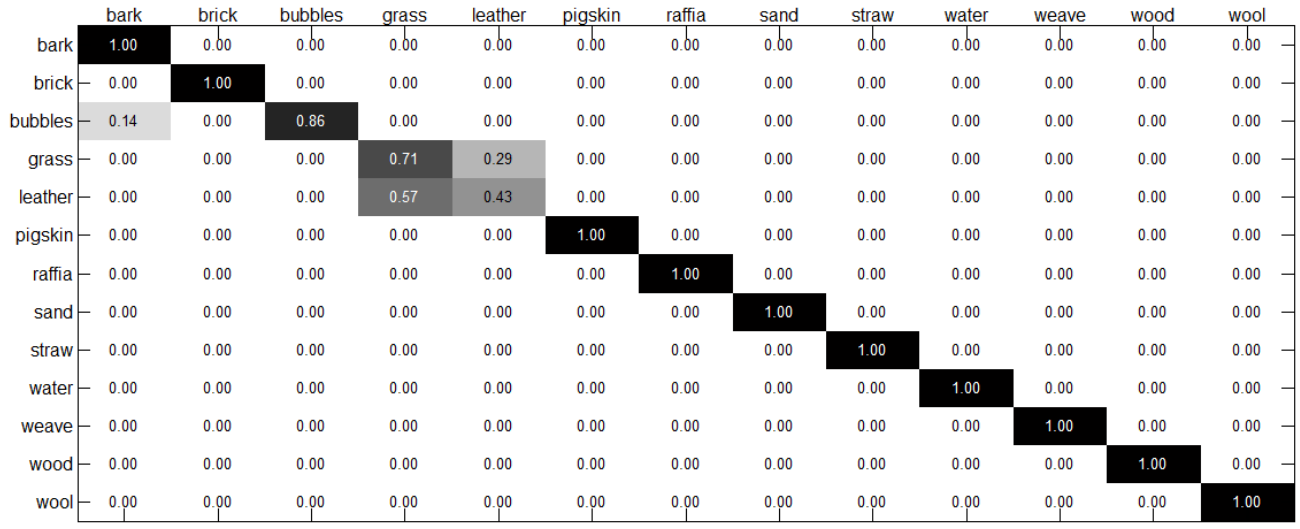

(b)

Figure 3. Performance comparison between (a) $LBP^{uni}_{P,R}$ and (b) $LBP^{uni}_{P,R} \backslash VAR_{P,R}$. In most cases, the variance information minimizes the error rate except for the "grass" class. In general, the variance information increases up to 12% the classification rate.

Downloaded from SPIE Digital Library on 03 May 2012 to 161.111.24.211. Terms of Use: http://spiedl.org/terms

The results can be summarized into three groups: *i*) LBPs based on minimal chains: LBP^{min}, $LBP^{min}_{P,R}$, and $LBP^{dom}_{P,R}$ compute a minimal chain. Their performance could be affected by noise because if a pixel intensity value is disturbed the final LBP label changes. *ii*) LBPs based on neighborhood values: Prior a LBP label computation, $LBP^{ni}_{P,R}$ and $LBP^{med}_{P,R}$ perform a weighted average of neighboring pixels to minimize the effects of noise. *iii*) LBPs based on uniform values: $LBP^{uni}_{P,R}$, $LBP^{num}_{P,R}$ compute a uniformity measure prior LBP label computation which corresponds to the number of spatial transitions in the pattern. Since $LBP^{num}_{P,R}$ add extra information of non-uniform patterns into the LBP histogram it has a better texture classification performance than $LBP^{uni}_{P,R}$.

Further work includes extending this techniques by applying a preprocessing stage based on Gabor filtering for increasing the robustness to illumination and noise degradations. Another extension will be based on the use of FPGAs to reduce the computational time.

ACKNOWLEDGMENTS

This work has been partially sponsored by the grant UNAM PAPIIT IN113611 and from the Spanish Ministry of Science and Technology the grants TEC2010-20307 and TEC2007-30709E. R. Nava gives a special thank to Consejo Nacional de Ciencia y Tecnología (CONACYT) for the doctoral scholarship 167161.

REFERENCES

[1] Mirmehdi, M., Xie, X., and Suri, J., [*Handbook of Texture Analysis*], Imperial College Press, London, UK (2009).

[2] Guo, Z., Zhang, L., Zhang, D., and Zhang, S., "Rotation invariant texture classification using adaptive LBP with directional statistical features," in [*17th IEEE International Conference on Image Processing (ICIP)*], 285–288 (2010).

[3] Davis, L. S., Johns, S. A., and Aggarwal, J. K., "Texture analysis using generalized co-occurrence matrices," *IEEE Transactions on Pattern Analysis and Machine Intelligence* **PAMI-1**(3), 251–259 (1979).

[4] Randen, T. and Husøy, J. H., "Filtering for texture classification: A comparative study," *IEEE Trans. Pattern Anal. Mach. Intell.* **21**(4), 291–310 (1999).

[5] Huang, D., Shan, C., Ardabilian, M., Wang, Y., and Chen, L., "Local Binary Patterns and its application to facial image analysis: a survey," *IEEE Transactions on Systems, Man, and Cybernetics, Part C: Applications and Reviews* **41**(6), 765–781 (2011).

[6] Nava, R., Escalante-Ramírez, B., and Cristóbal, G., "A comparison study of Gabor and log-Gabor wavelets for texture segmentation," in [*7th International Symposium on Image and Signal Processing and Analysis (ISPA)*], 189–194 (2011).

[7] Seetharaman, K., "Texture analysis based on a family of stochastic models," in [*IEEE International Conference on Signal and Image Processing Applications (ICSIPA)*], 518–523 (2009).

[8] Ojala, T., Pietikainen, M., and Harwood, D., "Performance evaluation of texture measures with classification based on Kullback discrimination of distributions," in [*Proceedings of the 12th International Conference on Pattern Recognition - Conference A: Computer Vision Image Processing (IAPR)*], **1**, 582–585 (1994).

[9] Wang, L. and He, D. C., "Texture classification using texture spectrum," *Pattern Recognition* **23**(8), 905–910 (1990).

[10] Zabih, R. and Woodfill, J., "Non-parametric local transforms for computing visual correspondence," in [*Proceedings of the third European conference on Computer Vision (Vol. II)*], 151–158, Springer-Verlag New York, Inc., Secaucus, NJ, USA (1994).

[11] Nanni, L., Brahnam, S., and Lumini, A., "Survey on LBP based texture descriptors for image classification," *Expert Systems with Applications* **39**(3), 3634–3641 (2012).

[12] Pietikäinen, M., Hadid, A., Zhao, G., and Ahonen, T., [*Computer vision using Local Binary Patterns*], vol. 40, Springer, 1st edition, xv, 207 p. 87 illus., 56 in color ed. (2011).

[13] Tan, X. and Triggs, B., "Enhanced local texture feature sets for face recognition under difficult lighting conditions," *IEEE Transactions on Image Processing* **19**(6), 1635–1650 (2010).

Downloaded from SPIE Digital Library on 03 May 2012 to 161.111.24.211. Terms of Use: http://spiedl.org/terms

[14] Ojala, T., Pietikäinen, M., and Maenpaa, T., "Multiresolution gray-scale and rotation invariant texture classification with local binary patterns," *IEEE Transactions on Pattern Analysis and Machine Intelligence* **24**(7), 971–987 (2002).

[15] Pietikäinen, M., Ojala, T., and Xu, Z., "Rotation-invariant texture classification using feature distributions," *Pattern Recognition* **33**(1), 43–52 (2000).

[16] Ma, Y., "Number local binary pattern: An extended local binary pattern," in [*2011 International Conference on Wavelet Analysis and Pattern Recognition (ICWAPR)*], 272 –275 (2011).

[17] Liu, L., Fieguth, P., and Kuang, G., "Generalized Local Binary Patterns for texture classification," in [*Proceedings of the British Machine Vision Conference*], 123.1–123.11, BMVA Press (2011).

[18] Fu, X. and Wei, W., "Centralized Binary Patterns embedded with image euclidean distance for facial expression recognition," in [*4th International Conference on Natural Computation*], **4**, 115–119 (2008).

[19] Tan, T., Zhang, M., and Liu, F., "Face recognition using Extended Local Binary Patterns and fuzzy information fusion," in [*7th International Conference on Fuzzy Systems and Knowledge Discovery (FSKD)*], **2**, 625–629 (2010).

[20] Guo, Z., Zhang, L., and Zhang, D., "A completed modeling of Local Binary Pattern operator for texture classification," *IEEE Transactions on Image Processing* **19**(6), 1657–1663 (2010).

[21] Liao, S., Law, M. W. K., and Chung, A. C. S., "Dominant Local Binary Patterns for texture classification," *IEEE Transactions on Image Processing* **18**(5), 1107–1118 (2009).

[22] Guo, Z., Zhang, L., and Zhang, D., "Rotation invariant texture classification using LBP variance (LBPV) with global matching," *Pattern Recognition* **43**(3), 706–719 (2010).

[23] Brodatz, P., "USC-SIPI," (Online; accessed 1 January 2012). `http://sipi.usc.edu/database/database.php?volume=rotate`.

[24] Brodatz, P., [*Textures; a photographic album for artists and designers*], Dover Publications, New York, USA (1966).

[25] Bishop, C. M., [*Pattern Recognition and Machine Learning (Information Science and Statistics)*], Springer-Verlag New York, Inc., Secaucus, NJ, USA (2006).

Downloaded from SPIE Digital Library on 03 May 2012 to 161.111.24.211. Terms of Use: http://spiedl.org/terms